

Solution Dynamics of Thallium–Metal Carbonyl Compounds Using ^{205}Tl NMR Spectroscopy

Jaap W. van Hal, Lawrence B. Alemany, and Kenton H. Whitmire*

Department of Chemistry, MS 60, Rice University, 6100 Main Street, Houston, Texas 77005-1892

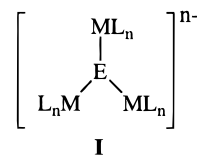
Received October 2, 1996[⊗]

A ^{205}Tl NMR study to probe the solution structure and dynamics of a series of thallium-containing metal complexes has been conducted. The following compounds were examined: $\text{Tl}\{\text{Co}(\text{CO})_4\}_3$ (**Ia**), $[\text{BnMe}_3\text{N}]_3[\text{Tl}\{\text{Fe}(\text{CO})_4\}_3]$ ($[\text{BnMe}_3\text{N}]_3[\text{Ib}]$), $\text{Tl}\{\text{M}(\text{CO})_3\text{Cp}\}_3$ (**Ic**, $\text{M} = \text{Cr}$; **Id**, $\text{M} = \text{Mo}$; **Ie**, $\text{M} = \text{W}$), TlFp_3 (**If**; $\text{Fp} = \text{CpFe}(\text{CO})_2$), $[\text{PPN}]_2[\text{Tl}_2\text{Fe}_6(\text{CO})_{24}]$ ($[\text{PPN}]_2[\text{III}]$), $[\text{Et}_4\text{N}]_2[\text{Tl}_2\text{Fe}_4(\text{CO})_{16}]$ ($[\text{Et}_4\text{N}]_2[\text{IIII}]$), $[\text{Et}_4\text{N}][\text{L}_2\text{Tl}\{\text{Fe}(\text{CO})_4\}_2]$ ($[\text{Et}_4\text{N}][\text{IV}]$: **IVa**[−], $\text{L}_2 = \text{bipy}$; **IVb**[−], $\text{L}_2 = \text{en}$; **IVc**[−], $\text{L}_2 = \text{phen}$; **IVd**[−], $\text{L}_2 = \text{tmeda}$; **IVe**[−], $\text{L}_2 = \text{dien}$), $[\text{Et}_4\text{N}]_4[\text{Tl}_4\text{Fe}_8(\text{CO})_{30}]$ ($[\text{Et}_4\text{N}]_4[\text{V}]$), and $\text{TlCo}(\text{CO})_4$ (**VI**). The ^{205}Tl NMR technique was used to probe the dynamic behavior of the Tl–metal cluster complexes $[\text{III}]^{2-}$, $[\text{IIII}]^{2-}$, and $[\text{V}]^{4-}$ in solution and the formation of Lewis base adducts of $[\text{III}]^{2-}$, as well as the possibility of formation of carbonylate anion adducts of **Ia**, **Ic**, **Id**, and **If**. **IVb**[−] reacted with acetone and formed, after fortuitous oxidation, $[\{(\text{CO})_4\text{FeL}_2'\text{Tl}\}_2\text{Fe}(\text{CO})_4]$ ($\text{L}_2' = \text{Me}_2\text{C}=\text{NCH}_2\text{CH}_2\text{N}=\text{CMe}_2$) (**VII**). The initially formed complex $[\text{L}_2'\text{Tl}\{\text{Fe}(\text{CO})_4\}_2]^{2-}$ ($[\text{Et}_4\text{N}][\text{IVf}]$) was spectroscopically characterized. Additionally, the two known but structurally uncharacterized complexes **Ia** and **If** as well as the new complexes $[\text{BnMe}_3\text{N}]_3[\text{Ib}]$ and **VII** were characterized by single-crystal X-ray diffraction. Compound **Ia** crystallizes in the monoclinic space group $P2_1/n$ with $a = 16.855(3)$ Å, $b = 6.7790(10)$ Å, $c = 19.049(4)$ Å, $\beta = 113.84(3)^\circ$, $V = 1990.8(6)$ Å³, $Z = 4$, $R_1(F) = 0.0221$, and $wR_2(F^2) = 0.0542$ [$I > 2\sigma(I)$]. Compound **If** was synthesized from $\text{K}[\text{Fp}]$ and $\text{TlCl}_3 \cdot 4\text{H}_2\text{O}$ and crystallizes in the triclinic space group $P\bar{1}$ with $a = 10.789(2)$ Å, $b = 14.239(3)$ Å, $c = 16.703(3)$ Å, $\alpha = 69.39(3)^\circ$, $\beta = 89.50(3)^\circ$, $\gamma = 69.07(3)^\circ$, $V = 2223.1(7)$ Å³, $Z = 4$, $R_1(F) = 0.0350$, and $wR_2(F^2) = 0.0877$ [$I > 2\sigma(I)$]. Compound $[\text{BnMe}_3\text{N}]_3[\text{Ib}]$ was synthesized from $\text{Na}_2\text{Fe}(\text{CO})_4 \cdot 3/2$ diox and $\text{Tl}(\text{OAc})_3$ in MeCN and crystallizes in the hexagonal space group $P6_3/m$ with $a = 18.290(3)$ Å, $c = 8.479(2)$ Å, $V = 2456.4(8)$ Å³, $Z = 2$, $R_1(F) = 0.0235$, and $wR_2(F^2) = 0.0494$ [$I > 2\sigma(I)$]. Compound **VII** crystallizes in the triclinic space group $P\bar{1}$ with $a = 13.597(3)$ Å, $b = 15.040(3)$ Å, $c = 10.536(2)$ Å, $\alpha = 92.75(3)^\circ$, $\beta = 95.07(3)^\circ$, $\gamma = 114.40(3)^\circ$, $V = 1946.0(7)$ Å³, $Z = 2$, $R_1(F) = 0.0461$, and $wR_2(F^2) = 0.1295$ [$I > 2\sigma(I)$].

Introduction

^{205}Tl is one of the more receptive nuclei that can be studied by NMR (relative receptivity compared to an equal number of protons = 0.19). The studies performed on organothallium and inorganic thallium compounds show ^{205}Tl to be extremely sensitive to its chemical environment because of its large chemical shift range. For instance, Me_3Tl has a chemical shift of 5093 ppm,¹ while, at the other extreme, $[\text{Bu}_4\text{N}][\text{TlI}_4]$ gives a signal at -1732 ppm.² However, not many metal–thallium compounds have been studied by this technique. ^{205}Tl NMR was used to identify the cluster TlSn_8^{5-} in the en (en = 1,2-diaminoethane) extract of the alloy $\text{Na}_2\text{Sn}_2\text{Tl}_3$.³ More recently, this technique was used to identify the intermediates and reaction products that arose when $[\text{Pt}(\text{CN})_4]^{2-}$ was treated with $\text{Tl}(\text{CN})_3$. The main product was identified as $[(\text{NC})\text{TlPt}(\text{CN})_5]^{-}$.⁴ The technique has also been used to probe interactions between the fluorine atoms and Tl^+ ions in $\text{Tl}_2\text{Zr}(\text{OCH}(\text{CF}_3)_2)_6$.⁵ The presence of two naturally-occurring spin- $1/2$ nuclei for thallium (^{205}Tl , ^{203}Tl ; 70.5%:30.5%) makes the use of ^{205}Tl NMR spectroscopy potentially very powerful for studying compounds

with more than one Tl center as the various isotopomers should exhibit ^{205}Tl – ^{203}Tl coupling yielding information diagnostic of structure and dynamics. Previous work on thallium iron carbonylates indicated that dissociation occurs in solution;⁶ therefore, a study on a number of the compounds for which Tl–Tl coupling could be used in this context was undertaken. Furthermore, the Tl center in a number of metal complexes is three-coordinate (**I**) and should possess Lewis acid character which has also been probed *via* this technique.



$\text{E} = \text{Tl}^{3+}$: **Ia**, $\text{ML}_n = \text{Co}(\text{CO})_4^-$, $n = 0$
Ib, $\text{ML}_n = \text{Fe}(\text{CO})_4^{2-}$, $n = 3$
Ic, $\text{ML}_n = \text{Cr}(\text{CO})_3\text{Cp}^-$, $n = 0$
Id, $\text{ML}_n = \text{Mo}(\text{CO})_3\text{Cp}^-$, $n = 0$
Ie, $\text{ML}_n = \text{W}(\text{CO})_3\text{Cp}^-$, $n = 0$
If, $\text{ML}_n = \text{Fp}^-$, $n = 0$
 $\text{E} = \text{In}^{3+}$ **Ig**, $\text{ML}_n = \text{Fe}(\text{CO})_4^{2-}$, $n = 3$

Experimental Section

General Methods. Unless otherwise specified, all synthetic manipulations were performed either on a Schlenk line or in a drybox under an atmosphere of purified nitrogen using standard inert-

* To whom all correspondence should be addressed.

⊗ Abstract published in *Advance ACS Abstracts*, June 15, 1997.

- (1) Köppel, H.; Dallorso, J.; Hoffman, G.; Walther, B. *Z. Anorg. Allg. Chem.* **1976**, *427*, 24.
- (2) Glaser, J.; Hendrikson, U. *J. Am. Chem. Soc.* **1981**, *103*, 6642.
- (3) Wilson, W. L.; Rudolph, R. W.; Lohr, L. L.; Taylor, R. C.; Pyykkö, P. *Inorg. Chem.* **1986**, *25*, 1535.
- (4) Berg, K. E.; Glaser, J.; Read, M. C.; Toth, I. *J. Am. Chem. Soc.* **1995**, *117*, 7550.
- (5) Samuels, J. A.; Zwanziger, J. W.; Lobkovsky, E. B.; Caulton, K. G. *Inorg. Chem.* **1992**, *31*, 4046.

- (6) Whitmire, K. H.; Cassidy, J. M.; Rheingold, A. L.; Ryan, R. R. *Inorg. Chem.* **1988**, *27*, 1347.

atmosphere techniques.⁷ All solvents were distilled under nitrogen from the appropriate drying agents.⁸ Infrared spectra were obtained in 0.1 mm CaF₂ cells by using a Perkin-Elmer 1640 Fourier transform infrared spectrometer. CO analyses were performed using methodology reported elsewhere.⁹ The compounds Na₂Fe(CO)₄·^{3/2}diox,¹⁰ [CpFe(CO)₂]₂ (Fp dimer),¹¹ TiCo(CO)₄ (**VI**), Ti{Co(CO)₄}₃ (**Ia**), Ti{M(CO)₃Cp}₃ (**Ic**, M = Cr; **Id**, M = Mo; **Ie**, M = W),¹² [PPN][Co(CO)₄],¹³ KC₈,¹⁴ [PPN]₂[Ti₂Fe₆(CO)₂₄] ([PPN]₂[**III**]),¹⁵ [Et₄N]₂[Ti₂Fe₄(CO)₁₆] ([Et₄N]₂[**III**]), [Et₄N][L₂Ti{Fe(CO)₄]₂] ([Et₄N][**IV**]: [**IVa**]⁻, L₂ = bipyridine (bipy); [**IVb**]⁻, L₂ = 1,2-diaminoethane (ethylenediamine, en); [**IVc**]⁻, L₂ = phenanthroline (phen); [**IVd**]⁻, L₂ = tetramethylethylenediamine (tmeda); [**IVe**]⁻, L₂ = diethylenetriamine (dien)),¹⁶ [Et₄N]₄[Ti₄Fe₈(CO)₃₀] ([Et₄N]₄[**V**]),⁶ and [CpCr(CO)₃]₂¹⁷ were all synthesized by literature methods, except that KC₈ was used as the reducing agent in place of Na–Hg or Na–K amalgam and Ti₂O₃ as the thallium source. Other reagents, Ti(OAc)₃ (Acros), TiCl₃·4H₂O (Organometallics), [BnMe₃N]Cl (Janssen, Bn = benzyl), TiNO₃ (Acros/Strem), and [CpM(CO)₃]₂ (M = Mo, W) (Strem), were used as supplied. Room temperature ²⁰⁵Tl NMR spectra were recorded on a IBM/Bruker AF 300 spectrometer operating at 173 MHz (Rice University). A Bruker AC-300P operating at 173 MHz (Baker Performance Chemicals, Houston, TX) was used to obtain variable-temperature ²⁰⁵Tl spectra (188–300 K: [**III**]²⁻, [**III**]²⁻, [**IVc**]⁻, [**V**]⁴⁺ (in acetone-*d*₆) and [**IVb**]⁻ (in 1:1 MeCN-*d*₃/PrCN)). ¹H and ¹³C spectra were recorded on a Bruker AC-250 spectrometer, operating at 250 MHz for ¹H and 62.9 MHz for ¹³C. All ²⁰⁵Tl spectra were referenced to a dilute solution (17mM) of TiNO₃ in D₂O (δ = 0).¹⁸ The field settings for acetone-*d*₆ and MeCN-*d*₃ were determined by placing a coaxial capillary insert with the dilute aqueous TiNO₃ solution in a 5 mm tube with acetone-*d*₆ and MeCN-*d*₃, respectively. A pulse width of 9 μs, corresponding to a 30° pulse, and a 1 s relaxation delay were used during data acquisition. The spectral region between 0 and 1.5 MHz downfield was searched in 50 kHz increments with a spectral width setting of 62.5 kHz. Samples for ²⁰⁵Tl NMR were prepared in the drybox by dissolving at least 100 mg/mL in acetone-*d*₆ or MeCN-*d*₃ or by preparing a saturated solution. Even dilute samples needed only 128 transients per scan range to find a clear signal. Chemical shifts, once they were found, were confirmed by varying offset and spectral width. Spectra were then obtained using appropriate spectral widths and relaxation delays. The formation of carbonylate anion adducts was studied by comparing the ²⁰⁵Tl signals of compounds **Ia,c,d,f** with solutions of about an equal concentration with added excess anion of the corresponding starting material (*i.e.* [PPN][Co(CO)₄], [PPN][CpCr(CO)₃], [PPN][CpMo(CO)₃], and [PPN][Fp] (synthesized from KC₈, metal carbonyl dimer, and PPNCl)). A metallic precipitate formed upon the addition of the corresponding metal carbonylate anions to **I**, except for **Ia** for which no precipitate formed and the ²⁰⁵Tl signal did not change.

Synthesis of [BnMe₃N]₃[IIb**].** Na₂Fe(CO)₄·^{3/2}diox, 1.1 g, 3.0 mmol, was weighed into a 100 mL Schlenk flask and dissolved in a minimal amount of MeCN. Solid Ti(OAc)₃ (0.28 g, 1.0 mmol) was added to solution, which turned deep red in about 15 min. After 1 h, the solvent was removed *in vacuo*, and a solution of 1.0 g of [BnMe₃N]Cl in 50 mL of water (sparged with dinitrogen for 1/2 h) was added slowly. The crude product was filtered out, washed with water and ether, and dried *in vacuo*. It was extracted into 30 mL of MeCN, filtered, and precipitated with excess ether. The product can be further purified by slow diffusion of diisopropyl ether (dipe) into a saturated MeCN

solution. The compound is appreciably soluble only in MeCN. IR, cm⁻¹ (MeCN): 1984, 1925 (sh), 1850. NMR, ppm (MeCN-*d*₃): ¹H, 7.53 (br, phenyl protons), 4.42 (s, methylene group), 3.03 (s, methyl groups); ¹³C, 225.2, CO, 133.9, 131.8, 130.2, 128.7 (phenyl carbons), 70.4 (methylene carbon), 53.5 (methyl carbons). CO analysis: calc, 0.0101 mol of CO/g; found, 0.0100 mol of CO/g.

Synthesis of **If.** Fp dimer (1.06 g, 3 mmol) and KC₈ (1.6 g, excess) were weighed into a 100 mL Schlenk flask in the drybox. After addition of 50 mL of thf, the mixture was stirred for 1 h and filtered through dry, degassed Celite. Upon addition of 0.72 g of TiCl₃·4H₂O (1.8 mmol), the mixture turned deep red. After filtration through dry, degassed Celite, the solvent was removed *in vacuo*. The residue was dissolved in 20 mL of acetone, filtered once more through Celite, and layered carefully with several volumes of dry 2-propanol. Upon subsequent diffusion, a white precipitate formed on the side of the flask. This was removed by filtration and the solution was cooled to -20 °C, from which the pure compound was obtained as black crystalline chunks (yield 0.37 g, 27%). The compound is soluble in most organic solvents, only moderately soluble in hexanes, insoluble in water, and is only moderately stable in chloroform. IR, cm⁻¹ (toluene): 1985, 1954, 1918. NMR, ppm: ¹H (CDCl₃), 4.72 (d, ³J(²⁰⁵Tl–¹H) = 26 Hz); ¹³C (d₈-toluene), 212.8 (CO) (d, ²J(²⁰⁵Tl–¹³C) = 363 Hz), 81.8 (Cp) (d, ²J(²⁰⁵Tl–¹³C) = 3 Hz). CO analysis: calc, 8.16 × 10⁻³ mol of CO/g; found, 8.15 × 10⁻³ mol of CO/g.

Spectroscopic Characterization of [Et₄N][IVf**].** [Et₄N][**IVb**] (1.0 g) was weighed into a 50 mL Schlenk flask and was dissolved in 5 mL of acetone. After being stirred overnight, the solution was filtered to remove a small amount of orange precipitate, and the solvent was removed *in vacuo*. The solid was washed with Et₂O and dried further *in vacuo*. ¹H NMR (MeCN-*d*₃): 3.619 (s, 4H, (Me₂C=NCH₂)₂), 3.180 (q, 8H, NCH₂CH₃), 2.180 and 1.937 (s, 6H, (Me₂C=NCH₂)₂), 1.222 (t of t, 12H, NCH₂CH₃). ¹³C NMR (MeCN-*d*₃): 220.5 (CO), 172.7 ((Me₂C=NCH₂)₂), 53.2 ((Me₂C=NCH₂)₂), 53.2 (t, NCH₂CH₃), 29.4 and 20.4 ((Me₂C=NCH₂)₂), 7.76 (NCH₂CH₃). IR, cm⁻¹ (MeCN): 1982, 1963, 1885, 1658. During one of the attempts to grow single-crystals at -20 °C in MeOH, a few red crystals of [(CO)₄FeL₂Tl]₂·Fe(CO)₄ (L₂' = (Me₂C=NCH₂)₂ (**IX**)) were isolated. Attempts to repeat this synthesis or to design a rational route to the product have not yet been successful. During a repeat of this reaction, a monoclinic polymorph of [Et₄N]₂[**III**] was isolated, which was characterized by single-crystal X-ray diffraction. Crystallographic data can be found in Table 1.

X-ray Crystallography. All crystals selected for data collection were mounted on the tip of a glass fiber with epoxy resin. Data for all compounds was collected on a Rigaku AFC5S automated four-circle diffractometer using the TEXSAN 5.0 software package¹⁹ and were corrected for Lorentz/polarization effects. The data of **If**, [Et₄N]₂[**III**], and **VII** were corrected for absorption using ψ-scans. No absorption correction was applied for **Ia** as the crystal suddenly decayed toward the end of the data collection, and none was deemed necessary for [BnMe₃N]₃[**IIb**] as indicated by flat ψ-scans. Extinction was refined for **Ia** and **If** using the expression $F_c^* = kF_c[1 + (0.001F_c^2\lambda^3/\sin(2\theta))]^{-1/4}$. Data collection and refinement parameters are summarized in Table 1. Scattering factors were taken from the literature.²⁰ Structures were solved using the SHELXTL-PLUS package on a PC.²¹ Refinement on F^2 on all reflections except those with very negative F^2 was performed with SHELXL-93 on a PC.²² Weighted R -factors wR and all goodnesses of fit (S) are based on F^2 ; conventional R -factors R are based on F , with F set to zero for negative F^2 . R -factors based on F^2 are statistically about twice as large as those based on F . The weighting factor $w = [\sigma^2(F_o^2) + (aP)^2 + bP]^{-1}$, where $P = (F_o^2 + 2F_c^2)/3$, was refined for a and b . All non-hydrogen atoms for all structures except the carbon atoms of **Ia** were refined with anisotropic

(7) Shriver, D. F.; Drezdon, M. A. *The Manipulation of Air Sensitive Compounds*; Wiley: New York, 1986.

(8) Gordon, A. J.; Ford, R. A. *The Chemist's Companion*; John Wiley and Sons: New York, 1972.

(9) Bachman, R. E.; Whitmire, K. H. *Organometallics* **1993**, *12*, 1988.

(10) Finke, R. G.; Sorell, T. N. *Org. Synth.* **1980**, *59*, 102.

(11) King, R. B. *Organometallic Syntheses*; Academic Press: New York, 1965; Vol. 1.

(12) Burlitch, J.; Theyson, T. W. *J. Chem. Soc., Dalton Trans.* **1974**, 828.

(13) Ruff, J. K.; Sliantz, W. S. *Inorg. Synth.* **1975**, *15*, 84.

(14) Schwindt, M. A.; Lejon, T.; Hegedus, L. S. *Organometallics* **1990**, *9*, 2814.

(15) Cassidy, J. M.; Whitmire, K. H. *Inorg. Chem.* **1989**, *28*, 1432.

(16) Cassidy, J. M.; Whitmire, K. H. *Inorg. Chem.* **1989**, *28*, 1435.

(17) Mahaffy, C. A. L.; Pauson, P. L. *Inorg. Synth.* **1990**, *28*, 136.

(18) Hinton, J. F.; Metz, K. R.; Briggs, R. W. *Annu. Rep. NMR Spectrosc.* **1982**, *13*, 211.

(19) TEXSAN, *Single Crystal Structure Analysis Software 5.0*; Molecular Structure Corp.: The Woodlands, TX, 1990.

(20) *International Tables for X-ray Crystallography*; Kluwers Academic Publishers: Dordrecht, The Netherlands, 1992; Vol. C, Tables 4.2.6.8. and 6.1.1.4.

(21) Sheldrick, G. M. *SHELXTL PLUS PC 5.0*; Siemens Crystallographic Research Systems: Madison, WI, 1990.

(22) Sheldrick, G. M. *SHELXL-93*; University of Göttingen: Göttingen, Germany, 1993.

Table 1. Crystal Data Collection and Refinement Parameters

	compound				
	Ia	[Et ₄ N] ₂ [III]	If	[BnMe ₃ N] ₃ [IIb]	VII
empirical formula	C ₁₂ Co ₃ O ₁₂ Tl	C ₃₂ H ₄₀ Fe ₄ N ₂ O ₁₆ Tl ₂	C ₂₁ H ₁₅ Fe ₃ O ₆ Tl	C ₄₂ H ₄₈ Fe ₃ N ₃ O ₁₂ Tl	C ₂₈ H ₃₂ Fe ₃ N ₄ O ₁₂ Tl ₂
fw	717.28	1340.80	735.25	1158.75	1192.87
space group	<i>P</i> 2 ₁ / <i>n</i> (No. 14)	<i>P</i> 2 ₁ / <i>n</i> (No. 14)	<i>P</i> 1̄ (No. 2)	<i>P</i> 6 ₃ / <i>m</i> (No. 176)	<i>P</i> 1̄ (No. 2)
<i>a</i> , Å	16.855(3)	8.902(2)	10.789(2)	18.290(3)	13.597(3)
<i>b</i> , Å	6.7790(10)	21.405(4)	14.239(3)		15.040(3)
<i>c</i> , Å	19.049(4)	12.084(3)	16.703(3)	8.479(2)	10.536(2)
α, deg			69.39(3)		92.75(3)
β, deg			89.50(3)		95.07(3)
γ, deg			69.07(3)		114.40(3)
<i>V</i> , Å ³	1990.8(6)	2203.3(8)	2223.1(7)	2456.4(8)	1946.0(7)
<i>Z</i>	4	2	4	2	2
ρ (calc), Mg/m ³	2.393	2.021	2.197	1.567	2.036
μ(Mo Kα), mm ⁻¹	10.580	8.634	9.179	4.196	9.402
temp (K)	297(2)	223(2)	297(2)	297(2)	297(2)
radiation; λ, Å			Mo Kα; 0.7107		
<i>R</i> ^a indices (<i>I</i> > 2 σ(<i>I</i>))	<i>R</i> ₁ = 0.0221 w <i>R</i> ₂ = 0.0542	<i>R</i> ₁ = 0.0362 w <i>R</i> ₂ = 0.0926	<i>R</i> ₁ = 0.0350 w <i>R</i> ₂ = 0.0877	<i>R</i> ₁ = 0.0235 w <i>R</i> ₂ = 0.0494	<i>R</i> ₁ = 0.0461 w <i>R</i> ₂ = 0.1295
<i>R</i> ^a indices (all data)	<i>R</i> ₁ = 0.0304 w <i>R</i> ₂ = 0.0573	<i>R</i> ₁ = 0.0549 w <i>R</i> ₂ = 0.2255	<i>R</i> ₁ = 0.0500 w <i>R</i> ₂ = 0.0973	<i>R</i> ₁ = 0.0368 w <i>R</i> ₂ = 0.0533	<i>R</i> ₁ = 0.0568 w <i>R</i> ₂ = 0.1377
transm coeff	N/A	0.33–1.0	0.6–1.0	0.97–1	0.15–1
<i>a</i> , <i>b</i> from <i>w</i>	0.0135, 1.9697	0.0543, 4.6887	0.0311, 10.8311	0.0207, 0.0	0.0922, 3.06895

$$^a R_1 = \sum ||F_o| - |F_c|| / \sum |F_o|; wR_2 = \{ \sum [w(F_o^2 - F_c^2)^2] / \sum [wF_o^4] \}^{1/2}; w^{-1} = [\sigma^2(F_o^2) + (aP^2) + bP]; P = [(F_o^2) + 2(F_c^2)]/3.$$

displacement parameters. Hydrogen atoms of all structures were included in their calculated positions with, for **If** and **VII**, temperature factors set to 1.5 times the equivalent isotropic temperature factor of the attached methyl carbon and to 1.2 times for hydrogen atoms attached to all other types of carbon atoms, while the hydrogens for [BnMe₃N]₃[**IIb**] were refined with a common temperature factor.

The structure of **Ia** shows minor distortions from 3-fold symmetry with a mirror plane through the TiCO₃ plane. The bond parameters for the carbonyl ligands are all within the values expected for terminally bound CO. It is isostructural to In{Co(CO)₄}₃.²³

As per the isostructural In analogue, [BnMe₃N]₃[In{Fe(CO)₄}₃] ([BnMe₃N]₃[**IIg**]),²⁴ [BnMe₃N]₃[**IIb**] was initially refined in the space group *P*6₃ but with a complete set of Friedel pairs collected in order to be able to determine the correct absolute structure. This initial refinement of the structure in *P*6₃ showed a large correlation between several parameters, and the cation was so badly disordered that no suitable model with reasonable bond parameters and temperature factors could be found. The structure was therefore refined in the centric space group *P*6₃/*m*. The cation was refined at half-occupancy near the mirror plane with the phenyl ring constrained to be a regular hexagon. On the basis of the successful refinement in the centric space group, we believe this choice to be the better of the two. The Ti atom lies on a 3-fold axis, the iron atom and two of the unique CO ligands lie on the mirror plane, and one CO lies on a general position. The overall imposed symmetry is *3/m*.

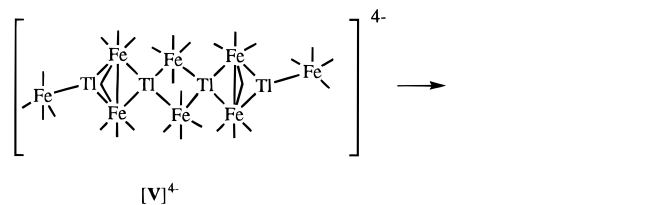
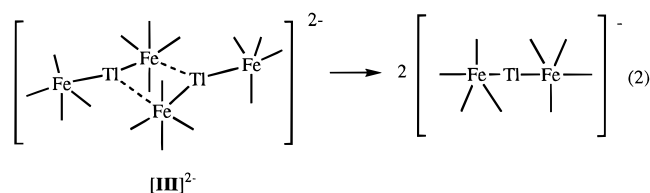
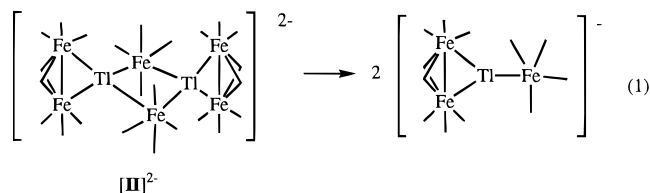
Compound **If** crystallizes with two molecules in the asymmetric unit and is isostructural and isomorphous to In{RuCp(CO)₂}₃.²⁵ Both unique molecules have the same conformation of the Cp rings with respect to the TiFe₃ plane: two up, one down. The conformation of the Cp rings is similar to the structure of GaFp₃²⁶ and Ti{CpMo(CO)₃}₃.²⁷ No crystal data are available for the InFp₃ structure.²⁸ The Fe–Cp and Fe–CO bond parameters are normal. The differences between the two unique molecules in the asymmetric unit are small. Two of the Cp rings of **If** were unstable upon initial refinement and were consequently constrained such that all the displacement factors in the direction of the 1,2 and 1,3 bonds in the ring were equal (DELU). Selected bond distances

for **Ia**, [BnMe₃N]₃[**IIb**], **If**, and **VII** are listed in Table 2. ORTEP projections are shown in Figures 2–4 and 6, respectively.

Results and Discussion

Solution Structure and Dynamics of Cluster Complexes.

As discussed in the introduction, any compound with more than one Ti atom should exhibit ²⁰⁵Tl–²⁰³Tl coupling, due to the presence of isotopomers. This phenomenon allows study of the dynamic behavior of the Ti–Fe bond of compounds such as [**II**]²⁻, [**III**]²⁻ and [**V**]⁴⁻ which could also undergo dissociation in solution as per eqs 1–3. Our previous work using ¹³C



(23) Robinson, W. R.; Schussler, D. P. *Inorg. Chem.* **1973**, *12*, 848.

(24) Albano, V. G.; Cané, M.; Iapalucci, M. C.; Longoni, G.; Monari, M. *J. Organomet. Chem.* **1991**, *407*, C9.

(25) Calabrese, J. C.; Clarkson, L. M.; Marder, T. D.; Norman, N. C.; Taylor, N. J. *J. Chem. Soc., Dalton Trans.* **1992**, 3525.

(26) Campbell, R. M.; Clarkson, L. M.; Clegg, W.; Hockless, D. C.; Pickett, N. L.; Norman, N. C. *Chem. Ber.* **1992**, *125*, 55.

(27) Rajaram, J.; Ibers, J. A. *Inorg. Chem.* **1973**, *12*, 1313.

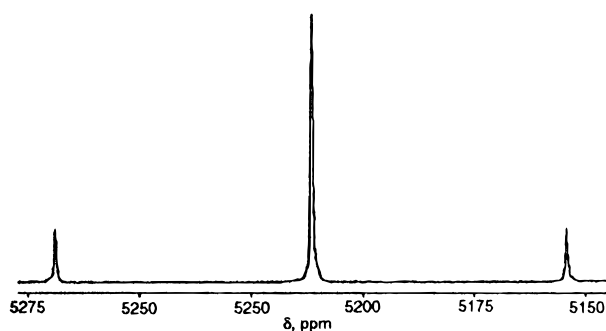
(28) Norman, N. C.; Webster, P. W. *Z. Naturforsch.* **1989**, *44b*, 91.

NMR spectroscopy had indicated that this was the case for [**III**]²⁻.⁶ To study to the dynamic behavior of these Ti–Fe

Table 2. Selected Bond Distances and Angles for **Ia**, **If**, [BnMe₃N]₃[**Ib**], and **VII**^a

Compound Ia			
Tl(1)–Co(2)	2.6480(14)	Tl(1)–Co(3)	2.6603(14)
Tl(1)–Co(1)	2.662(2)	Co–C range	1.75–1.80
Co(2)–Tl(1)–Co(3)	119.68(5)	Co(2)–Tl(1)–Co(1)	121.06(4)
Co(3)–Tl(1)–Co(1)	118.95(5)	Co(2)–Tl(1)–C(34)	127.7(2)
Co(3)–Tl(1)–C(34)	36.6(2)	Co–C–O range	172–178
Compound If , Molecule 1			
Tl(11)–Fe(13)	2.643(2)	Tl(11)–Fe(12)	2.644(2)
Tl(11)–Fe(11)	2.662(2)	Fe–C range	1.70–1.77
Fe–Cp(center) range	1.71–1.73		
Fe(13)–Tl(11)–Fe(12)	122.44(5)	Fe(13)–Tl(11)–Fe(11)	117.98(5)
Fe(12)–Tl(11)–Fe(11)	119.39(5)	Fe–C–O range	176–179
Compound If , Molecule 2			
Tl(21)–Fe(23)	2.638(2)	Tl(21)–Fe(22)	2.639(2)
Tl(21)–Fe(21)	2.650(2)	Fe–C range	1.73–1.74
Fe–Cp(center) range	1.72–1.73		
Fe(23)–Tl(21)–Fe(22)	121.63(5)	Fe(23)–Tl(21)–Fe(21)	119.25(5)
Fe(22)–Tl(21)–Fe(21)	118.97(5)	Fe–C–O range	176–179
Compound [BnMe ₃ N] ₃ [Ib]			
Tl(1)–Fe(1)#1	2.6940(12)	Tl(1)–Fe(1)#2	2.6940(12)
Tl(1)–Fe(1)	2.6940(12)	Fe–C range	1.71–1.77
Fe(1)#1–Tl(1)–Fe(1)#2	120.0	Fe(1)#1–Tl(1)–Fe(1)	120.0
Fe(1)#2–Tl(1)–Fe(1)	120.0	Fe–C–O range	175–180
Compound VII			
Tl(1)–N(41)	2.545(12)	Tl(1)–Fe(1)	2.578(2)
Tl(1)–N(42)	2.635(13)	Tl(1)–Fe(3)	2.700(2)
Tl(2)–N(52)	2.472(12)	Tl(2)–N(51)	2.538(13)
Tl(2)–Fe(2)	2.569(2)	Tl(2)–Fe(3)	2.749(2)
Fe–C range	1.70–1.85		
N(41)–Tl(1)–Fe(1)	107.7(3)	N(41)–Tl(1)–N(42)	67.7(4)
Fe(1)–Tl(1)–N(42)	103.3(3)	N(41)–Tl(1)–Fe(3)	102.7(3)
Fe(1)–Tl(1)–Fe(3)	147.91(7)	N(42)–Tl(1)–Fe(3)	97.5(3)
N(52)–Tl(2)–N(51)	69.1(4)	N(52)–Tl(2)–Fe(2)	112.7(3)
N(51)–Tl(2)–Fe(2)	107.4(3)	N(52)–Tl(2)–Fe(3)	102.0(3)
N(51)–Tl(2)–Fe(3)	111.5(3)	Fe(2)–Tl(2)–Fe(3)	134.95(8)
Fe–C–O range	173–179		

^a Symmetry transformations used to generate equivalent atoms: (#1) $-y + 1, x - y, z$; (#2) $-x + y + 1, -x + 1, z$.

**Figure 1.** ²⁰⁵Tl NMR spectrum of [III]²⁻.

bonds, first it had to be established that ²⁰⁵Tl–²⁰³Tl coupling could indeed be observed for these compounds. Compound [III]²⁻ was chosen as it was the least likely to dissociate in solution on the basis of the bond parameters for the central Tl₂Fe₂ ring structure.

For [III]²⁻ a triplet signal with the expected 3:14:3 ratio based on the 70.5:29.5 ratio of ²⁰⁵Tl:²⁰³Tl was observed with an isotope effect of -58 Hz or -0.3 ppm (digital resolution = 1.09 Hz) and is shown in Figure 1. The coupling constant of 19 835 Hz of compound [III]²⁻ is apparently the largest Tl–Tl ²J known (cf. ²J = 2560 Hz for [TlOEt₄]).²⁹ At 190 K this coupling constant has increased to 21 000 Hz, with a downfield shift in

the signal of 43 ppm, and the isotope effect is -65 Hz. The ²J coupling constants to ²⁰⁵Tl have been reported to change by 5–10% upon lowering the temperature.³⁰ Since the Tl–Tl distance in [III]²⁻ is 3.507(1) Å, which is only 0.1 Å longer than the distance in Tl metal (3.40 Å),^{31,32} one could argue that this is in fact a ¹J coupling. Coupling between metal atoms can be very large; for instance, the ¹J(¹⁹⁹Hg–¹⁹⁹Hg) in [Hg₃][AsF₆] is 139.6 kHz³³ and the ²J(¹¹⁷Sn–¹¹⁹Sn) in *trans*-[Pd(SnCl₃)₂(AsEt₃)₂] is 37.2 kHz.³⁴ From the magnitude alone, no definitive answer about the order of the coupling in [III]²⁻ can be given. The Tl–Fe–Tl angle of 79.11(4)^o and short Tl–Tl distance are consistent with a large two-bond coupling through a short Fermi contact. Since the ²⁰⁵Tl spectrum shows these couplings, it can be concluded that the compound does not dissociate in solution. The isotope effect is to our knowledge the first example of an observable ²⁰⁵Tl–²⁰³Tl isotope effect and is at least 1 order of magnitude larger on a ppm basis than, for example, the isotope effect caused by substituting ¹³C for ¹²C on the ¹³C chemical shift of a ¹³C–¹²C pair. Since the magnitude of the isotope effect is a reflection of the chemical shift range, the order of magnitude is not entirely unexpected.³⁵

Anion [III]²⁻ (eq 2) shows a singlet and, on the basis of chemical shifts and lack of Tl–Tl coupling, probably exists as the monomeric [Tl{Fe(CO)₄}₂]⁻ in solution, although the line width could obscure coupling. The absence of any observable coupling in [III]²⁻ suggests even more strongly that the compound is indeed dissociated in solution as previously postulated on the basis of IR and ¹³C NMR spectroscopy; the solution IR spectrum of [III]²⁻ shows a simple, symmetrical two-band pattern, similar to other LFe(CO)₄ compounds. In contrast, the solid-state infrared spectrum (KBr pellet) shows considerably broader features with shoulders and humps indicative of a number of additional CO environments ($\nu_{\text{CO}} = 1995$ (sh), 1990, 1940 (sh), 1920 (sh), 1895, 1880 cm⁻¹). Likewise, the solution ¹³C spectrum shows only one signal. If the solid-state structure of [III]²⁻ were retained in solution, a more complex ν_{CO} pattern in the infrared spectrum and at least two signals in the ¹³C spectrum would be expected.⁶ The only differences in the spectrum at RT (room temperature) and 190 K were the upfield shift (764 ppm) and the sharpening of the ²⁰⁵Tl signal. The large shift in the ²⁰⁵Tl NMR signal could result from a change in the coordination number for Tl (*vide infra*) with lower temperatures. A reasonable postulate is that solvent coordination is occurring to produce a [Tl(acetone)_x{Fe(CO)₄}₂]⁻ species at lower temperatures. (Note that at room temperature there is no difference in the CO-stretching region of the IR spectra of the compound in potentially coordinating solvents such as acetone compared to spectra in classically “noncoordinating” solvents such as CH₂Cl₂.) The -50 °C polymorph of [III]²⁻, isolated during one of the attempts to synthesize VII, has similar bond distances and angles as the room temperature polymorph reported earlier.⁶ The only significant differences are the Tl–Fe bond distances in the planar Tl₂Fe₂ unit (Tl–Fe

(29) Schneider, W. G.; Buckingham, A. D. *Disc. Farad. Soc.* **1962**, 34, 147.

(30) Hinton, J. F.; Metz, K. R.; Briggs, R. W. *Prog. NMR Spectrosc.* **1988**, 20, 423.

(31) Wells, A. F. *Structural Inorganic Chemistry*; Oxford University Press: London, 1975.

(32) Wyckoff, R. W. G. *Crystal Structures*, 2; Interscience Publishers: New York, 1963; Vol. 1.

(33) Gillespie, R. J.; Granger, P.; Morgan, K. R.; Schrobilgen, G. J. *Inorg. Chem.* **1984**, 23, 887.

(34) Starzewski, K. H. A. O.; Pregosin, P. S.; Ruegger, H. *Helv. Chim. Acta* **1982**, 65, 785.

(35) Jameson, C. J. In *Encyclopedia of Nuclear Magnetic Resonance*; Grant, D. M., Harris, R. K., Eds.; John Wiley: New York, 1996; Vol. 4, p 2638.

2.632(5) and 3.038(4) Å, with Tl–Tl–Fe 80.0(1)° for the RT structure *vs* Tl–Fe 2.6101(14) and 3.237(2) Å, with Tl–Tl–Fe 80.29(4) for the –50 °C polymorph) making the dimer even more asymmetrical than the room-temperature structure.

Compound **[V]**^{4–} shows a triplet with approximately the same relative intensities as compound **[III]**^{2–} but with a much smaller coupling constant; however, the breadth of the signals makes an accurate relative integration impossible. No isotope effect was detectable (digital resolution = 3.05 Hz) in this case. No other signals were detected within 200 kHz of the triplet. Compound **[V]**^{4–} can be viewed as a dimer of two [Fe₂(CO)₇{TiFe(CO)₄}₂]^{2–} units. The bond parameters suggest much stronger bonding between the monomeric units than in **[III]**^{2–}. If this dimer form for compound **[V]**^{4–} were retained in solution, a very complicated pattern would be expected, since the compound would have nine unique isotopomers, of which seven contain both ²⁰³Tl and ²⁰⁵Tl. A coupling pattern consistent with the dissociation into a species such as [Fe₂(CO)₇{TiFe(CO)₄}₂]^{2–} units containing two Tl nuclei, however, is observed. The smaller coupling constant as compared to **[III]**^{2–} is in agreement with the longer Tl···Tl distances found in the solid-state structure of [Et₄N]₄[**V**] (3.859(2) Å), assuming that no significant changes in the structure within the monomeric unit occur upon dissociation. By 188 K (the low-temperature limit of acetone-*d*₆), the triplet has started to collapse and has shifted about 170 ppm to higher field, while a new signal at 5851 ppm begins to form. At this temperature, the peaks are still broad and no coupling is discernible. The signal at 5851 ppm is in the region of four-coordinate Tl (*vide infra*), which suggests that the dimer could be starting to aggregate at this temperature. A peak would still be expected in the region of 6000 to 6600 ppm, as **[V]**^{4–} possesses both four- and three-coordinate Tl centers. Due to limited solubility of [Et₄N]₄[**V**] in lower freezing solvents, this phenomenon could not be further pursued.

Lewis Acid Adducts. Three coordinate E{ML_n}₃ complexes and the monomer derived from **[III]**^{2–} are all formally electron deficient at Tl and would be expected to serve as Lewis acid centers. This has been proven for **[III]**^{2–} with the isolation of several chelating base adducts of the form [L₂Tl{Fe(CO)₄}₂][–] (L₂ = bipy, en, phen, tmeda, dien),¹⁶ and a literature report described [Tl{Co(CO)₄}₄][–] but structural confirmation was lacking.³⁶ The known E{ML_n}₃ possess trigonal planar coordination at Tl as expected by VSEPR theory. This is confirmed for **Ia, f**, which were previously uncharacterized by single-crystal diffraction (Table 2). This confirmation was important for **Ia**, which shows an anomalous chemical shift compared to other compounds in this series. While the synthesis of compound **If** might be expected to be straightforward, there was a significant challenge associated with its separation from byproduct Fp₂, which has similar solubility properties. After extensive trials it was found that the Fp dimer could be removed by fractional crystallization from acetone/2-propanol. Also during the course of this investigation the new trigonal planar compound [BnMe₃N]₃[**Ib**] was synthesized. Compound [BnMe₃N]₃[**Ib**] formed in moderate yield from Collman's reagent and Ti(OAc)₃. All attempts to make the compound in a similar procedure as for **[Ig]**^{3–},²⁴ using Collman's reagent and TiCl₃, failed. In addition, using a Tl/Fe ratio of 1:3 in the KOH/MeOH/Fe(CO)₅ system only yielded **[III]**^{2–} and a metallic precipitate, presumably Tl. The ¹H spectrum of [BnMe₃N]₃[**Ib**] shows only signals assignable to the cation, while the ¹³C spectrum shows, in addition to peaks for the cation, one singlet for the carbonyl ligands, consistent with the "breadth" of the ²⁰⁵Tl signal. The

Table 3. Ambient ²⁰⁵Tl NMR Data

compd	δ (ppm)	ν _{1/2} (LB) ^a (Hz)	coupling ⁿ J(²⁰⁵ Tl–X) (Hz)
Ia	4009	800 (10)	
[Ib] ^{3–}	6032	100 (10)	
Ic	6032	220 (10)	
Id	6082	100 (10)	
If	6523	~8 (1)	³ J(²⁰⁵ Tl– ¹ H) = 26; ² J(²⁰⁵ Tl– ¹³ Cp) = 3; ² J(²⁰⁵ Tl– ¹³ CO) = 363 ² J(²⁰⁵ Tl– ²⁰³ Tl) = 19 835
[III] ^{2–}	5213	85 (5)	
[III] ^{2–}	6626	1200 (43)	
[III] ^{2–b}	6549	4850 (173)	
[IVa] [–]	~4700	~85 kHz (173)	
[IVa] ^{–b}	~5050	~60 kHz (173)	
[IVb] [–]	"4767"	9400 (173)	
[IVb] ^{–b}	4516	1240 (10)	
[IVc] [–]	4733	4700 (173)	
[IVc] ^{–b}	4680	3400 (10)	
[IVd] [–]	5768	8100 (173)	
[IVd] ^{–b}	5677	19.6 kHz (173)	
[IVe] ^{–b}	4372	160 (1)	
[V] ^{4–}	6778	280 (10)	² J(²⁰⁵ Tl– ²⁰³ Tl) = 1920
VI	1558	310 (10)	

^a LB = line broadening used in data processing. ^b Measured in MeCN-*d*₃.

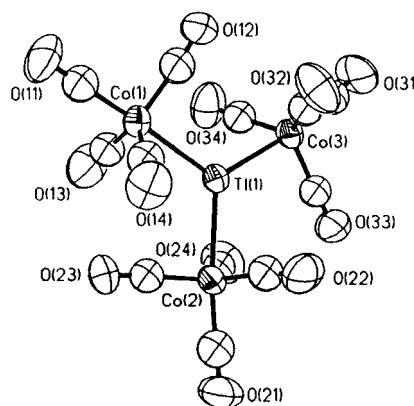


Figure 2. ORTEP projection of **Ia** (50% probability). The carbon atoms are labeled according to their attached oxygen atoms.

IR spectrum shows a simple three-band pattern, as is commonly found for molecules with trigonal bipyramidal Fe(CO)₄ groups. The Tl–Fe distances of **[Ib]**^{3–} (2.6940(12) Å) are longer than the short Tl–Fe distances in **[III]**^{2–} (2.553(5) and 2.632(5) Å), are in the range of the Tl–Fe distances in **[V]**^{4–} (2.530(7)–2.718 Å) and [Et₄N]₆[Ti₆Fe₁₀(CO)₃₆] ([Et₄N]₆[**VIII**]) (2.540(4)–2.790(4) Å),⁶ but are shorter than those in **[III]**^{2–} (2.746(2)–2.765(2) Å).¹⁵

The Lewis acid behavior of these complexes was probed further in solution *via* ²⁰⁵Tl NMR spectroscopy. The electron-deficient three-coordinate compounds **[Ib]**^{3–}, **Ic**, **Id**, **If**, and **[V]**^{4–} as well as **[III]**^{2–} all have ²⁰⁵Tl signals in the range from 6000 to 6800 ppm (Table 3). The three-coordinate nature of Tl (see structure **I**) for these compounds in the solid state was confirmed for **Ia**, **[Ib]**^{3–}, and **If** by single-crystal X-ray crystallography. Compound **Ia** (Figure 2) has the most shielded nucleus of all Tl(III) compounds in this study, lying well upfield of the other trigonal planar complexes examined here. The source of this shift is not apparent as **Ia** is isoelectronic and isostructural to the other compounds in this series having similar M–Tl bond distances. The ²⁰⁵Tl spectrum of compound **[Ib]**^{3–} (Figure 3) is a singlet and, as expected, is less deshielded than **[III]**^{2–}, consistent with the less electron deficient nature of **[Ib]**^{3–} compared to dissociated **[III]**^{2–}. From the difference in chemical shift (~600 ppm) and from the different line width

(36) Robinson, W. R.; Schussler, D. P. *J. Organomet. Chem.* **1971**, *30*, C5.

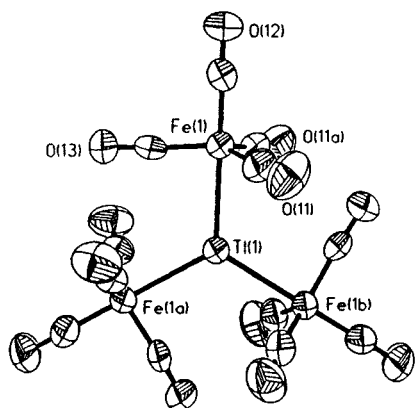


Figure 3. ORTEP projection of $[\text{Ib}]^{3-}$ (50% probability). The carbon atoms are labeled according to their attached oxygen atoms.

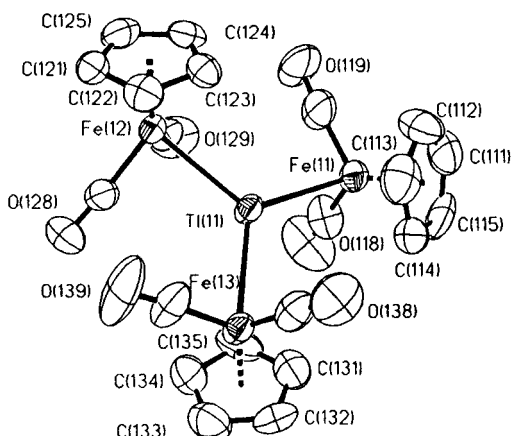


Figure 4. ORTEP projection of **If** (50% probability). The carbon atoms are labeled according to their attached oxygen atoms.

compared to $[\text{III}]^{2-}$, it was obvious that the synthesis of $[\text{Ib}]^{3-}$ had been successful and that the compound retains all three iron atoms in solution. The signals of **Ic,d,f** were also found in the same region and are very deshielded as expected for these neutral “electron-deficient” molecules. Due to its limited stability, no NMR signal could be obtained for compound **Ie**. Compound **If** (Figure 4) shows a complex pattern (at least 10 lines resolved), and its spectrum along with a simulation is shown in Figure 5. The falloff of intensities fits the binomial distribution for coupling to 15 equivalent protons. The doublet with the same J value for the Cp rings in the ^1H spectrum supports this interpretation of the ^{205}Tl spectrum. The ^{13}C spectrum shows a doublet for the carbonyl signals ($^2J(^{205}\text{Tl}-^{13}\text{C}) = 363\text{ Hz}$), with shoulders on the inside that are probably due to $^{13}\text{C}-^{203}\text{Tl}$ coupling [$\gamma(^{203}\text{Tl})/\gamma(^{205}\text{Tl}) = 0.990$]. The Cp region in the ^{13}C spectrum shows a doublet with a small $^{205}\text{Tl}-^{13}\text{C}$ coupling constant. A similar phenomenon has also been found in $(\text{CO})_x\text{WCp}$ type compounds, for which no $^{13}\text{C}-^{183}\text{W}$ coupling to the Cp ring was observed, and also in the absence of $^{31}\text{P}-^{13}\text{C}$ coupling to the Cp ring in $(\text{CO})_x\text{FeCp}(\text{phosphine})$ type compounds (but coupling to the CO was observed).³⁷ The pattern in the carbonyl stretching region of the IR is a three-band pattern, similar to the pattern found for $\text{In}\{\text{CpRu}(\text{CO})_2\}_3$.²⁵

The effect of complexation on the ^{205}Tl signal was examined for the series of known chelating base adducts. Broad featureless signals were obtained for $[\text{Et}_4\text{N}][\text{IV}]$, evidenced by the line widths which clearly indicated the presence of quadrupolar nitrogen atoms bonded to the thallium. Further indication of this relaxation mechanism stems from the sharpening of the

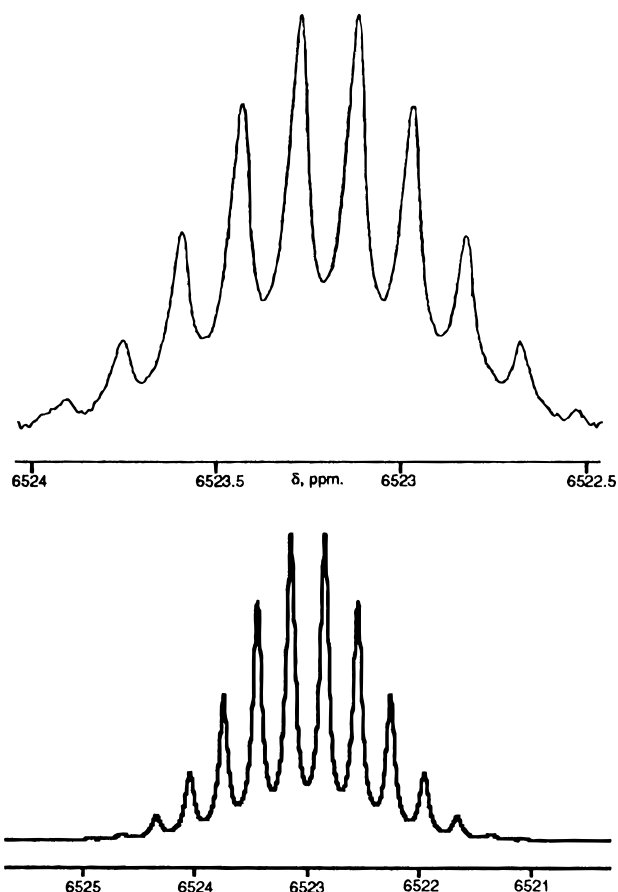
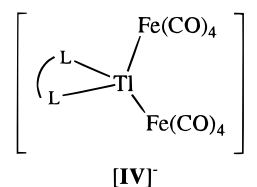


Figure 5. Observed (top) and simulated (bottom) ^{205}Tl NMR spectrum of **If**. The spectrum was simulated with a line width of 8 Hz, $\delta = 6523$, and $J = 26\text{ Hz}$.

signal of $[\text{IVc}]^-$ at 188 K, an observation in agreement with literature precedent.³⁸ In addition, the chemical shifts indicate a less deshielded Tl environment than the parent $[\text{III}]^{2-}$, as expected due to the higher electron count at Tl in the former compounds. Reinvestigation of the ^{13}C and ^1H NMR signals clearly show no coupling to the ^{205}Tl , which is in agreement with the width of the ^{205}Tl signal, making the proton and carbon experiments effectively decoupled for ^{205}Tl , as is also seen in the ^{13}C spectrum of $[\text{Ib}]^{3-}$.



- [IVa]⁻**: $\text{L}_2 = \text{bipy}$
[IVb]⁻: $\text{L}_2 = \text{en}$
[IVc]⁻: $\text{L}_2 = \text{phen}$
[IVd]⁻: $\text{L}_2 = \text{tmEDA}$
[IVe]⁻: $\text{L}_2 = \text{dien}$

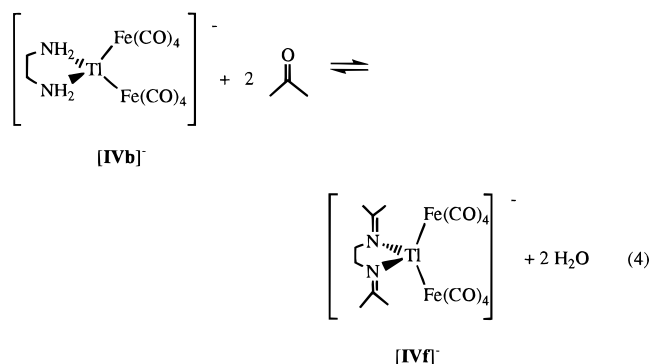
The ^{205}Tl signal for compound $[\text{Et}_4\text{N}][\text{IVb}]$ shifted during the data acquisition at room temperature due to the reaction of the coordinated en with acetone- d_6 (*vide infra*), and so the NMR spectra of appropriate salts of $[\text{III}]^{2-}$ – $[\text{IVe}]^-$ were also obtained in $\text{MeCN}-d_3$ to facilitate comparison. ^{13}C signals have been

(37) Mann, B. E.; Taylor, B. F. *^{13}C NMR Data for Organometallic Compounds*; Academic Press: New York, 1981.

(38) Roe, D. C. In *Experimental Organometallic Chemistry*; Wayda, A. L., Darensbourg, M. Y., Eds.; American Chemical Society: Washington, DC, 1987; Vol. 357, p 204.

correlated to various ligand parameters. For instance, the ^{13}C shift of the series $\text{Fe}(\text{CO})_4(\text{phosphine})$ and $\text{Fe}(\text{CO})_3(\text{phosphine})_2$ could be correlated to the Tolman χ -parameter of the phosphine.^{39–41} However, no obvious correlation could be found between the ^{205}Tl chemical shift and common parameters for ligands such as the Jørgensen parameter f , which quantifies the spectrochemical series.⁴² This is probably due to the magnitude of the range of chemical shifts for ^{205}Tl , where small subtle changes in the Tl environment cause large differences in the chemical shift. For instance, the difference in Jørgensen parameters f for phen and dien (0.05) is small (values range from 0.72 for Br^- to 1.7 for CN^-), while the chemical shift difference is about 300 ppm. This large chemical shift value, however, only represents a small percentage of the Tl chemical shift range. The difference between the Tolman χ -parameters for the different phosphines is about 30 giving rise to a 3 ppm difference in ^{13}C shifts of the CO ligand. However, the pairs of Tl compounds with the most similar ligands, $[\text{IVa}]^-$ and $[\text{IVc}]^-$, as well as $[\text{IVb}]^-$ and $[\text{IVe}]^-$, show similar chemical shifts, and the signal for $[\text{IVd}]^-$ is much more deshielded than $[\text{IVb}]^-$. This is in agreement with the diminished ligand strength of tmeda with respect to en in terms of f . Unfortunately, the en adduct has eluded structural characterization, and so a more definitive discussion based upon bond distance comparison is not possible. The relatively small shifts in the ^{205}Tl NMR signals when changing from acetone- d_6 to MeCN- d_3 indicate that the solvent has relatively small influence on the environment around the Tl(I) ion shift was previously found to be at least 2600 ppm and can be attributed to solvent–thallium bonding, which presumably does not occur for these compounds.⁴³

^{13}C NMR analysis of a solution of $[\text{IVb}]^-$ in acetone- d_6 indicated the presence of an imine. Reproduction of the conditions in the NMR tube with protioacetone yielded a compound whose spectroscopic properties are in agreement with the formation of $[(\text{Me}_2\text{C}=\text{NCH}_2)_2\text{Ti}\{\text{Fe}(\text{CO})_4\}_2]^-$ ($[\text{IVf}]^-$) (eq 4). Both the solution of $[\text{IVb}]^-$ in acetone- d_6 and $[\text{IVf}]^-$ have



signals assignable to imine carbons in the ^{13}C -NMR spectrum. The presence of two seven-line patterns in the baseline in the ^{13}C -NMR spectrum of $[\text{IVb}]^-$ in acetone- d_6 at approximately the same shifts as the methyl signals of $[\text{IVf}]^-$ in MeCN- d_3 supports the assignment of these signals in $[\text{IVb}]^-$ to CD_3 groups. It also clearly identifies acetone as the source for the

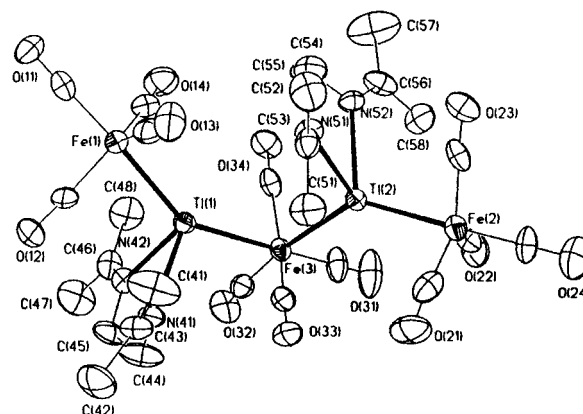


Figure 6. ORTEP projection of **VII** (30% probability). The carbon atoms of the carbonyls are labeled according to their attached oxygen atoms.

imine formation. In addition, the shifts match the spectroscopic properties reported for $\text{L}'\text{Mo}(\text{CO})_4$ reasonably well.⁴⁴ The initially-formed complex is extremely moisture sensitive, in agreement with water-scavenging properties of the ligand reported earlier.⁴⁵

The reaction between acetone and $[\text{IVb}]^-$ was also probed by adding 3 equiv of acetone to a solution of $[\text{IVb}]^-$ in MeCN- d_3 . The ^{205}Tl signal shifted and became much broader; however, only signals assignable to $[\text{IVb}]^-$ and acetone were observed when the condensation reaction was followed by ^1H NMR over a 12-h period. During the same time frame, about half of the en had reacted with solvent acetone in the control experiment. In that experiment, about an equal concentration of en (with respect to $[\text{IVb}]^-$) was treated with acetone in MeCN- d_3 . The shift in the ^{205}Tl NMR signal upon addition of acetone to a MeCN- d_3 solution of $[\text{IVb}]^-$ is probably due to subtle changes in the dielectric properties. The only change observed in the ^{205}Tl spectrum at 190 K of a solution of $[\text{IVb}]^-$ and acetone in 1:1 MeCN- d_3 and PrCN was sharpening and a shift of the signal. The reaction to form the diimine, therefore, appears to require high concentrations of acetone to drive the apparent equilibrium (eq 4) toward the right side. This formation of a diimine has been proposed as one of the intermediates in the formation of various N_4 -macrocycles from metal-bound N_2 -ligands and ketones and also explains the moisture sensitivity of the product.⁴⁶

During one of many unsuccessful attempts to grow single-crystals of $[\text{Et}_4\text{N}][\text{IVf}]$, $[\{(\text{CO})_4\text{FeL}_2'\text{Ti}\}_2\text{Fe}(\text{CO})_4]$ ($\text{L}_2' = (\text{Me}_2\text{C}=\text{NCH}_2)_2$, **VII**) was formed apparently after fortuitous oxidation. While this was not the desired product, the structural analysis (Figure 6), however, did confirm the production of the diimine ligand. Compound **VII** is insoluble in most organic solvents and was only obtained once in very low yield despite numerous attempts to duplicate the reaction conditions. While quite a few complexes with diimine ligands derived from acetone are known, **VII** is the first metal complex that is crystallographically characterized with the ligand (Cambridge Crystallographic Data Base as of Dec 1996). The Tl–Fe distances of the terminal iron atoms are comparable to those found in $[\text{IV}]^-$,¹⁶ while those for the bridging iron are similar to those found for $[\text{III}]^{2-}$.¹⁵ The Tl–Fe and Tl–N distances are in the same range as those found earlier in the Lewis base adducts of $[\text{III}]^{2-}$.¹⁶

(39) Gansow, O. A.; Vernon, W. D. In *Topics in Carbon-13 NMR Spectroscopy*; Levy, G. C., Ed.; John Wiley and Sons: New York, 1976; Vol. 2.

(40) Nieche, E.; Gudaf, D. In *Phosphorus-31 NMR Spectral Properties in Compound Characterization and Structural Analysis*; Quin, L. D., Verkade, J. G., Eds.; VCH: New York, 1994.

(41) Whitmire, K. H.; Lee, T. R. *J. Organomet. Chem.* **1985**, 282, 95.

(42) Jørgensen, C. K. *Modern Aspects of Ligand Field Theory*; Elsevier: New York, 1971.

(43) Dechter, J. J. *Prog. Inorg. Chem.* **1982**, 29, 285.

(44) Paz-Sandoval, M. A.; Domínguez-Durán, M. E.; Pzaos-Mayen, C.; Ariza-Castolo, A.; de Jesús Rosales-Hoz, M.; Contreras, R. *J. Organomet. Chem.* **1995**, 492, 1.

(45) Holm, R. T. *J. Paint Technol.* **1967**, 39, 385.

(46) Curtis, N. F. In *Comprehensive Coordination Chemistry*; Wilkinson, G., Ed.; Pergamon: Oxford, U.K., 1987; Vol. 2.

Attempts were also made to probe the formation of Lewis base adducts with excess metal carbonylate anions. No change in the ^{205}Tl signal was observed upon addition of anions to solutions of **Ia**, **c**, **d**, **f**, and only **Ia** did not form metallic precipitate upon addition of the metal carbonylate anion. This seems to contradict earlier findings which indicated reaction between **Ia** and $[\text{Co}(\text{CO})_4]^-$.³⁶ On the other hand, the reaction of $[\text{Co}(\text{CO})_4]^-$ with $\text{In}\{\text{Co}(\text{CO})_4\}_3$ in the presence of $[\text{Et}_4\text{N}]\text{I}$ yielded $[\text{Et}_4\text{N}]\text{I}\{\text{In}\{\text{Co}(\text{CO})_4\}_3\}$.⁴⁷

Conclusions

^{205}Tl NMR provides a convenient spectroscopic handle to make structural assignments and observe dynamic solution behavior, especially for complexes with more than one Tl center. On the basis of observed coupling patterns, it was possible to examine dissociation of aggregates in solution. Most metalated compounds where Tl is formally three-coordinate generally gave signals in the region between 6000 and 6800 ppm, whereas all

compounds where Tl is formally four-coordinated gave signals in the region between 4400 and 5800 ppm. Many of the ^{205}Tl chemical shifts observed are significantly downfield of those previously reported.

Acknowledgment. This work was assisted by a grant from the Robert A. Welch Foundation and the National Science Foundation (Grant CHE-9408613). We gratefully acknowledge Mr. James A. Hackerott of Baker Performance Chemicals Inc. for his assistance with the VT studies and Dr. Charles F. Harper for making the instrument available to us. We also wish to thank Dr. William K. Wilson for his assistance in simulating the ^{205}Tl spectrum.

Supporting Information Available: Plots of representative ^{205}Tl NMR spectra including acquisition parameters (5 pages). X-ray crystallographic files, in CIF format, for the structures **Ia**, $[\text{BnMe}_3\text{N}]_3[\text{Ib}]$, **If**, the monoclinic polymorph of $[\text{Et}_4\text{N}]_2[\text{III}]$, and **VII** are available on the Internet only. Access and ordering information is given on any current masthead page.

(47) Clarkson, L. M.; Farrugia, L. J.; Norman, N. C. *Acta Crystallogr.* **1991**, *C47*, 2525.